A Sliding Mode Controller Approach for Three Phase Single Stage Seven Level Multilevel Inverter for Grid Connected Photovoltaic System

K. Rajasekhara Reddy*‡, V. Nagabhaskar Reddy **, M.Vijaya Kumar ***

*Research Scholar, JNTUA, Ananthapuramu & Assistant Professor, Department of EEE, Santhiram Engineering College, Nandyal, A.P, India,

**Professor & Head, Department of EEE, Rajeev Gandhi Memorial College of Engg. & Tech. Nandyal, A.P, India

***Professor, Department of EEE & Registrar, JNTUA, Ananthapuramu, A.P, India

(raju.gprec@gmail.com, vnbr_ndl@yahoo.co.in, mvk_2004@rediffmail.com)

‡Corresponding Author; K. Rajasekhara Reddy, Jawaharlal Nehru Technological University Anantapur, Ananthapuramu, A.P, India. Tel: +91 9951000912. raju.gprec@gmail.com

Received: 27.08.2020 Accepted:25.09.2020

Abstract- This paper brought out the interest of eliminating a dc-dc converter stage in a two stage power conversion system to reduce the complexity, size and cost. The problem of the paper is formulated from the observations made by the existing literature, which have very less scope about the elimination of dc-dc converter stage in power conversion system.It is proposed and evaluated by implementing the combinations of the proportional Integral and sliding mode controllers to evaluate the grid side parameters such as grid voltage and current, real power, reactive power, power factor and dc link voltage settling time for standard atmospheric condition and changing atmospheric condition. Existing inverter topologies have the drawbacks in the terms of number of levels to reduce the harmonics and dc link voltage maintenace for the disturbances caused at grid side and source side. The proposed system is analysed by implementing a three phase seven level diode clamped multilevel inverter. A multiloop controller is designed as the inner loop controls the power factor and the outerloop track the maximum power from photovoltaic syatem. This paper finally arrives at a conclusion about the stastical and simulated results of the proposed system by using MATLAB/SIMULINK.

Keywords- Photovoltaic System; Seven Level Diode Clamped Inverter; Proportional Integral, Sliding Mode Controller; Standard Atmospheric Condition; Changing Atmospheric Condition.

Nomenclature:

N_{ll}	Number of cells in parallel	R	Line Resistance
N_{sl}	Number of cells in series	L	Line Inductance
I_{DS}	Saturation Current	γ_m	Switching States
v_{pv}	PV array output voltage in volts/dc link voltage	l	Level of the inverter
i_{pv}	PV array output current in amps	S_Ψ	Sliding Surface
I_{LG}	Light generating current source	P_S	Apparent Power
I_{DS}	Shunt diode current in amps	P_R	Real Power
R_{se}	Series Resistance in ohms	P_Q	Reactive Power
R_{sh}	Shunt Resistance in ohms	i_d ,i_q	Direct and Quadrature Currents
u_m	Phase voltages	sgn	Sigmoid Function
i_m	Line currents	v_d ,v_q	Control Vectors
e_{gm}	Grid voltages	T	Time

1. Introduction

Increasing energy requirements in industrial applications, solar energy is one of the most commonly used forms in renewable energy. Owing to the rapid growth of solar cell technology, performance and reliability have been enhanced in recent years. Solar and wind energy, unlike fossil fuels, are inexhaustible and clean sources of energy in nature[1-3]. Photovoltaic (PV) applications are now categorized into two types: First, standalone applications need energy storage by the battery bank and are used for low-power applications such as residential applications. Second, a PV network with a grid connection where full power is extracted and injected into the grid and the power factor stays nearly unity, even as environment varies. On the other side, solar energy relies heavily on various environmental influences, mainly solar radiation and atmospheric temperature[4-6]. Current and voltage of the PV array are the function of solar irradiation and cell temperature. PV Current varies with radiation, and the evolution of the temperature follows PV voltage[36]. A power electronic circuit is acts as an interface between PV panels and utility grid and is necessary to transfer the maximum power[7-8].

There are two technologies used in energy handling for power transfer from a Photovoltaic (PV) module to the grid: (i) a two-stage power conversion in which the grid is linked into the PV system via a dc-dc converter to boost the voltage working on Maximum Power Point Tracker (MPPT) and a DC-AC Power Factor Correction (PFC) and conversion device, and (ii) Single-stage power transfer with direct DC-AC conversion, where it can act as both operations like to Maximum Power Point (MPP) and PFC[9-10]. A voltage control loop is used to control the dc link voltage, for this a PV terminal voltage is required. To model the MPPT [34-35] a PV voltage and currents are needed in single stage grid connected PV system. A single stage grid connected PV system enhances the system efficiency by eliminating the dc-dc converter. It is also enhances the voltage and current profile under the different operating conditions at source side and grid side[11-12].

The grid-connected PV system proposes a single-stage power conversion to reduce circuit complexity and power loss. A power converter as a conventional Seven-level Diode Clamped Multi-Level Inverter (SDC-MLI) topology is proposed and used for an interfacing device in between PV and grid-connected system[13-15].

The inverters are generally classified as three types based on the mode of operation. Stand-alone, Grid connected and Bimodal inverters. Stand-alone inverters are also called as off-grid inverters, these are used to convert dc voltage of PV system in to ac and it supplies stable voltage and frequency to the load. Grid connected inverters are further classified as the central inverter, string inverter, multi string inverter and module integrated inverters. These are discussed in the reference of [31].Bimodal inverters are very expensive and these are used in less often.

The PV system has nonlinear electrical behavior due to changes in solar irradiation and the temperature and disturbs the smooth working of the inverter operation. However, there are different types of linear controllers such as proportional integral controller, predictive controller, hysteresis controller etc. In [16-17], the performance of these controllers on nonlinear PV systems should not give the satisfactory response at all operating points as well for the continuous changes in atmospheric conditions. Nevertheless, it provides adequate service at a series of operating points, since the system is linearized at a balance stage[18-20]. The limits of linear controllers are overcome through the introduction of non-linear controllers for non-linear PV systems to operate under all working conditions and atmospheric conditions. A model predictive based nonlinear PID controller stated in [21-23] . A Lyapunov-based controller is included in [24-25] for grid-connected PV inverter, and The law on adaptation is included in order to improve robustness.

In order to satisfy the following criteria, a proportional integral- Sliding Modes Controller (PI-SMC) is introduced, one to control and derive the maximum power from the PV system and secondly for PFC to provide a grid voltage, and the currents are spaced in order to achieve a Unity PF[16],[32].

This paper mainly focuses on,

- In order to reduce the size of the filter and resonance problems, a diode clamped multilevel inverter of seven level is proposed and evaluated.
- A comparative analysis is carried out by implementing the following controller combinations of PI-SMC.
- Evaluation of proposed system is done by considering Standard Atmospheric Conditions and Changing Atmospheric Condition.
- It is also considered and evaluated about the performance while occurrence of fault at grid side.
- Statically it is proved that combination of sliding mode controller and proportional integral at inner and outer loops are outstanding.

2. Power System Configuration and Modeling:

Power system configuration split into different sections as a PV panel, SDC-MLI with dc link capacitor and the electrical grid. PV system interfaced with SDC-MLI, a small passive filter connected at the Inverter output to handle the harmonics and connected to the grid, as shown in Fig.1. The operation of SDC-MLI discussed in [29] with Phase Disposition Multicarrier based Pulse Width Modulation (PDMC-PWM).

In diode clamped multilevel inverter, for the generation of multilevel output voltage it employs (l-1)*(l-2) clamping diodes and (l-1) dc link capacitors connected. The three phase SDC-MLI as shown in Fig.1., it represents the 30 numbers of clamping diodes and 6 numbers of dc link capacitors are connected for splitting of dc link voltage v_{pv} into v_{pv} /6 to generate the required output voltage. In SDC-MLI, can be synthesized by taking the neutral point N as a reference, for phase voltage $V_{AN} = +v_{pv}/2$ is obtained by conducting a positive group of switch S_{a1}-S_{a6}, for $+v_{pv}/3$, the switches S_{a2}-S_{a6} from positive group and S_{a1}' from negative group. The switching states and phase voltage levels for leg A are illustrated in Table 1 and is considered from [29]. In which '1'

stands for switch is on and "0" for switch off. The required components for SDC-MLI is illustrated in [29].

2.1. PV System Configuration:

There are several models in various literature, such as the single diode, double diode and three diode model and so on, which illustrate the nonlinear behavior of the PV system. Among these, a single model diode and double model diode are usually used because they are easily analyzed and implemented as well as a minor error with respect to the characteristics of solar PV cells[37]. In this paper, a mathematical equation for modeling of single model diode is preferred and is taken from[3], [27]. In order to meet the maximum power in the PV system, an Incremental Conductance method[34] is used as a MPPT and is addressed [26-27].

$$i_{pv} = N_{ll}I_{LG} - N_{ll}I_{DS}\left[e^{A\left(\frac{v_{pv}}{N_{sl}}+\frac{i_{pv}R_{se}}{N_{ll}}\right)} - 1\right] - \left[\frac{N_{ll}^2 v_{pv} + N_{ll}N_{sl}(i_{pv}R_{se})}{N_{ll}N_{sl}R_{sh}}\right] \quad (1)$$

2.2. Power System Modeling:

When design in power system model, consider a grid side of the three-phase inverter and can be written in terms of voltages and current with passive filters elements as[24-25],

$$u_m = Ri_m + L\frac{di_m}{dt} + e_{gm}, \ \ where, m = a, b, c \quad (2)$$

Where, u_m are the phase voltages, i_m are the currents flowing into the grid, e_{gm} are the grid voltages, R are the line resistance and L are the line inductance.

Equation (2) can be expressed as,

$$\frac{di_m}{dt} = -\frac{R}{L}i_m - \frac{e_{gm}}{L} + \frac{u_m}{L} \quad (3)$$

Equation (3) is discussed in reference [5],[7]

The phase voltage u_m [30] can be expressed in terms of input switching states γ_m for SDC-MLI, then,

$$[u_m]_{3X1} = \frac{1}{3} * \frac{v_{pv}}{(l-1)}\begin{bmatrix} 2 & -1 & -1 \\ -1 & 2 & -1 \\ -1 & -1 & 2 \end{bmatrix}_{3X3} [\gamma_m]_{3X1} \quad (4)$$

Where, l = level of the inverter

From the equation (3) & (4),

$$\left[\frac{di_m}{dt}\right]_{3X1} = \begin{bmatrix} -\frac{R}{L} & 0 & 0 \\ 0 & -\frac{R}{L} & 0 \\ 0 & 0 & -\frac{R}{L} \end{bmatrix}_{3X3} [i_m]_{3X1} + \begin{bmatrix} -\frac{1}{L} & 0 & 0 \\ 0 & -\frac{1}{L} & 0 \\ 0 & 0 & -\frac{1}{L} \end{bmatrix}_{3X3} [e_{gm}]_{3X1} + \frac{v_{pv}}{18L_m}\begin{bmatrix} 2 & -1 & -1 \\ -1 & 2 & -1 \\ -1 & -1 & 2 \end{bmatrix}_{3X3} [\gamma_m]_{3X1} \quad (5)$$

The dc link voltage v_{pv} from the model is expressed as[5],[7],[33]

$$\dot{v_{pv}} = \frac{1}{c}i_{pv} - \frac{1}{c}(\gamma_a i_a + \gamma_b i_b + \gamma_c i_c) \quad (6)$$

Equation (5) & (6) are nonlinear and time varying models, these are transform into time invariant model by using $adc - dq0$ transformation.

Therefore,

$$\begin{cases} \dot{I_d} = -\frac{R}{L}I_d + \omega I_q - \frac{e_{gd}}{L} + \frac{v_{pv}}{6L}\gamma_d \\ \dot{I_q} = -\omega I_d - \frac{R}{L}I_q - \frac{e_{gq}}{L} + \frac{v_{pv}}{6L}\gamma_q \\ \dot{v_{pv}} = \frac{1}{C}i_{pv} - \frac{1}{C}I_d\gamma_d - \frac{1}{C}I_q\gamma_q \end{cases} \quad (7)$$

Equation (7) is used to design control input vectors for SMC [7].

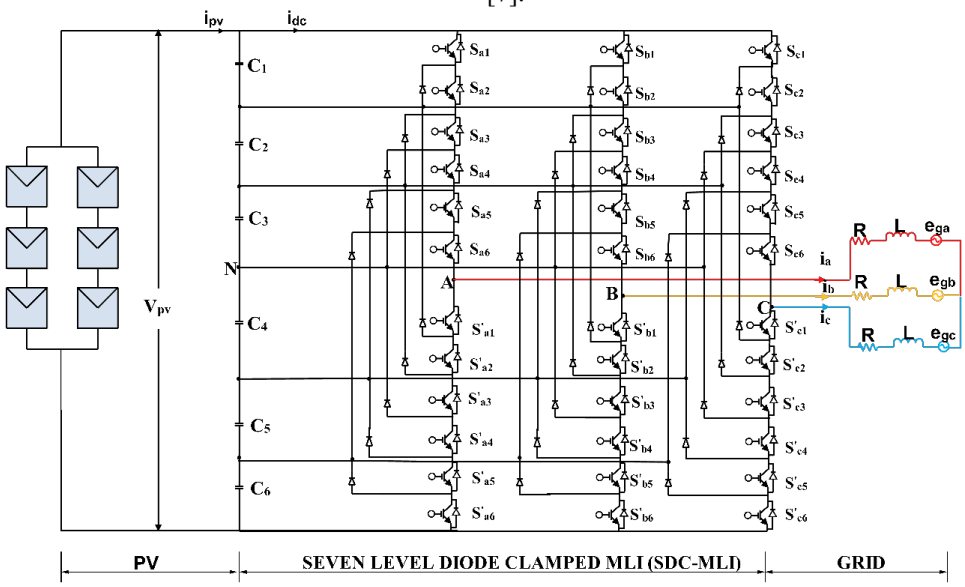

Fig.1. Single stage seven level diode clamped MLI with grid interfaced PV system [26]

Table 1. Switching states of **leg A** for SDC-MLI [26]

Switching function for Leg 'A'	Switching State	Output
S_a	(Sa_1, Sa_2, Sa_3, Sa_4, Sa_5, Sa_6=1 and Sa_1', Sa_2', Sa_3', Sa_4', Sa_5', Sa_6'=0)	$+V_{pv}$
	(Sa_1', Sa_2, Sa_3, Sa_4, Sa_5, Sa_6=1 and Sa_1, Sa_2', Sa_3', Sa_4', Sa_5', Sa_6'=0)	$+2V_{pv}/3$
	(Sa_1', Sa_2', Sa_3, Sa_4, Sa_5, Sa_6=1 and Sa_1, Sa_2, Sa_3', Sa_4', Sa_5', Sa_6'=0)	$+V_{pv}/3$
	(Sa_1', Sa_2', Sa_3', Sa_4, Sa_5, Sa_6=1 and Sa_1, Sa_2, Sa_3, Sa_4', Sa_5', Sa_6'=0)	0
	(Sa_1', Sa_2', Sa_3', Sa_4', Sa_5, Sa_6=1 and Sa_1, Sa_2, Sa_3, Sa_4, Sa_5', Sa_6'=0)	$-V_{pv}/3$
	(Sa_1', Sa_2', Sa_3', Sa_4', Sa_5', Sa_6=1 and Sa_1, Sa_2, Sa_3, Sa_4, Sa_5, Sa_6'=0)	$-2V_{pv}/3$
	(Sa_1', Sa_2', Sa_3', Sa_4', Sa_5', Sa_6'=1 and Sa_1, Sa_2, Sa_3, Sa_4, Sa_5, Sa_6=0)	$-V_{pv}$

3. Designing of sliding mode controller:

Sliding Mode Controller (SMC) is used to get excellent performance, robustness and fast dynamic response under the external disturbances and significant variations in system parameters. The sliding mode can be described as a state trajectory evolution of a system that contains the specified hyper plane (switching surface) with a stable dynamics of a state space. In the design of SMC have to carry two steps, the primary step is to design a sliding surface such that it satisfies the sliding motion in precise design specifications, i.e., the dynamic behavior of the system is configured by the sliding surface (S_Ψ). Secondly, the establishment of an appropriate control law that directs the closed loop system to the sliding surface to handle the uncertainties, including external disruption, nonlinearity and model parameter uncertainties.
The non-linear SMC mathematical model can be represented by the following equation[17-18],

$$\dot{x}(t) = f(x,t) + g_1(x,t)v(t) \quad (8)$$
$$y\,(t) = c(x,t) \quad (9)$$

Where, t is the time ($\epsilon\ \mathbb{R}$), $x \epsilon \mathbb{R}^n$ is the state vector,y and v are the output and input variables and f and g are the vector fields. It is assume [28] that the input variable $v(x,t)$ experiences a discontinuity on the surface ($S_\Psi\ (x,t) = 0$), then [35],

$$v(x,t) = \begin{cases} v^+(x,t) & is\ S_\Psi\ (x,t) > 0 \\ v^-(x,t) & is\ S_\Psi\ (x,t) < 0 \end{cases} \quad (10)$$

When the system is in sliding mode, the standardized sliding surface can be described as follows [35]:

$$S_\Psi\ (x,t) = 0\ \ and\ \ \dot{S_\Psi}\ (x,t)\ = 0,\ \forall t\ \geq t_0 \quad (11)$$

Where, t_0 is time reached for sliding mode (S_Ψ)
Substituting equation (8) in equation (11), then,

$$\dot{S_\Psi}\ (x,t) = \frac{\partial S_\Psi}{\partial x}\ \dot{x} = \frac{\partial S_\Psi}{\partial x}[f(x,t) + g(x,t)v(t)] = 0 \quad (12)$$

The control inputs $v(t)$ can be expressed as [22],

$$v(t) = -\left[\left[\frac{\partial S_\Psi}{\partial x}\right]\ g(x,t)\right]^{-1}\left[\frac{\partial S_\Psi}{\partial x}\ [f(x,t)]\right] \quad (13)$$

Substitute equation (13) in equation (8), then the system dynamics on the sliding surface is,

$$\dot{x}(t) = \left[I -\ g(x,t)\left[\left[\frac{\partial S_\Psi}{\partial x}\right]\ g(x,t)\right]^{-1}\frac{\partial S_\Psi}{\partial x}\right] f(x,t) \quad (14)$$

Once the dynamics of the system is fixed, then define the control law for the state trajectory on the sliding surface and is described by [21],

$$v = -Vsgn(S_\Psi) \quad (15)$$

Where, V is constant positive value and sgn is sigmoid function.

The PV system connected to the grid supplies the maximum power in the grid, so the complex power supplied is expressed as,

$$P_S = P_R + jP_Q \quad (16)$$

Where, P_S , P_R and P_Q are is an apparent power, real power and reactive power.

The P_R and P_Q are expressed by using Park Transformation[18]

Therefore,

$$P_R = \frac{3}{2}\left(e_{gd}i_d + e_{gq}i_q\right)$$
$$P_Q = \frac{3}{2}\left(e_{gq}i_d - e_{gd}i_q\right) \quad (17)$$

Where, e_{gd} and e_{gq} are the grid voltage component along with d and q-axis and i_d ,i_q are the direct and quadrature component of the currents. From the equation (17), the P_R and P_Q are depends on both d and q-axis quantities, so independent control of P_R and P_Q are complex. Assume that, the grid

voltage component e_{gd} is made zero, then P_R and P_Q expressed as,

$$\begin{aligned} P_R &= \frac{3}{2}\left(e_{gq} i_q\right) \\ P_Q &= \frac{3}{2}\left(e_{gq} i_d\right) \end{aligned} \tag{18}$$

The sliding surface defined by using current dynamic error ($e_j = i_d^{ref} - i_d$). However, we can also add an integral terms to improve the performance accuracy as shown equation (19),

Generally[35],

$$S_{\Psi j} = e_j + c_i \int e_j . dt \tag{19}$$

$where,\ j = d, q\ and\ i = 1,2,3 \ldots$

From equation (19), the sliding surface for inner current loop is expressed as[21],

$$\begin{vmatrix} S_{\Psi d} = i_d^{ref} - i_d + c_1 \int_0^t \left(i_d^{ref} - i_d\right) dt \\ S_{\Psi q} = i_q^{ref} - i_q + c_2 \int_0^t \left(i_q^{ref} - i_q\right) dt \end{vmatrix} \tag{20}$$

The i_d^{ref} and i_q^{ref} are the reference proportions of d-and q-axis and are expressed as,

$$\begin{vmatrix} i_d^{ref} = \frac{2}{3}\frac{P_Q^{ref}}{u_d} \\ i_q^{ref} = \frac{2}{3}\frac{P_R^{ref}}{u_q} \end{vmatrix} \tag{21}$$

Assume that the reactive power reference P_Q is zero when at unity PF, therefore the equation (21) becomes,

$$\begin{vmatrix} i_d^{ref} = 0 \\ i_q^{ref} = \frac{2}{3}\frac{P_R^{ref}}{u_q} \end{vmatrix} \tag{22}$$

The control vectors v_d and v_q can be composed for SMC for grid connected PV system as [21],

$$v_j = v_{jequ} + v_{jnl}, where,\ j = d, q \tag{23}$$

Where $v_{jequ}$the equivalent control input that extracts the system behavior on the sliding surface and v_{jnl} are the nonlinear inputs that drive the state to the sliding surface and retain the state on the sliding surface with system parametric uncertainties.

Therefore, the control input vectors, based on equation (23), for SMC for three phase grid connected PV system is expressed as[21],

$$\begin{bmatrix} v_d \\ v_q \end{bmatrix} = \begin{bmatrix} Ri_d + \omega L i_q + e_{gd} + c_1 L\left(i_d^{ref} - i_d\right) \\ Ri_q - \omega L i_d + e_{gq} + c_2 L\left(i_q^{ref} - i_q\right) \end{bmatrix} + \begin{bmatrix} V_1 sgn(S_{\Psi d}) \\ V_2 sgn(S_{\Psi d}) \end{bmatrix} \tag{24}$$

Where,

$$\begin{bmatrix} v_{dequ} \\ v_{qequ} \end{bmatrix} = \begin{bmatrix} Ri_d + \omega L i_q + e_{gd} + c_1 L\left(i_d^{ref} - i_d\right) \\ Ri_q - \omega L i_d + e_{gq} + c_2 L\left(i_q^{ref} - i_q\right) \end{bmatrix};$$

$$\begin{bmatrix} v_{dnl} \\ v_{qnl} \end{bmatrix} = \begin{bmatrix} V_1 sgn(S_{\Psi d}) \\ V_2 sgn(S_{\Psi d}) \end{bmatrix} \tag{25}$$

4. Results and discussion:

In PV integrated power system, stability is an essential factor if any change in irradiation and temperature, so, maintenance of constant DC input voltage for SDC-MLI is needed even any changes in operating characteristics of the plant. The conventional Proportional Integral-Proportional Integral (PI-PI) controller operating with fixed parameters but can't ensure the stability with these parameters in a system, even though the robust nonlinear input-output partial feedback controller [27] improve the power quality but it has few limitations while in designing. Hence, PI-SMC is proposed in this paper, and it will enhance the system stability at all operating conditions. The complete operating structure of the PI-SMC based SDC-MLI single stage grid-connected PV system, as shown in Fig.2. In this system, it is necessary to design two control loops one is to track the maximum power point is called voltage control loop, and second loop for maintain the unity power factor for better power quality is called current control loop, is designed using equation (24). In Fig.2. PI-SMC is arranged as follows, PI controller used as an outer loop and SMC is placed in an inner loop and same is comapred with conventional PI (outer loop)-PI (inner loop) controller combination. The performance of PI-SMC is validated by comparing PI-PI controller in simulation results and numerical values. In ac side, the output voltages and currents with linear elements are transforms into $adc - dq0$ for analysis of control law and then re-tranform into $dq0 - abc$ and is used to generate pulses by taking a PDMC-PWM methodology for SDC-MLI to maintain system stability.

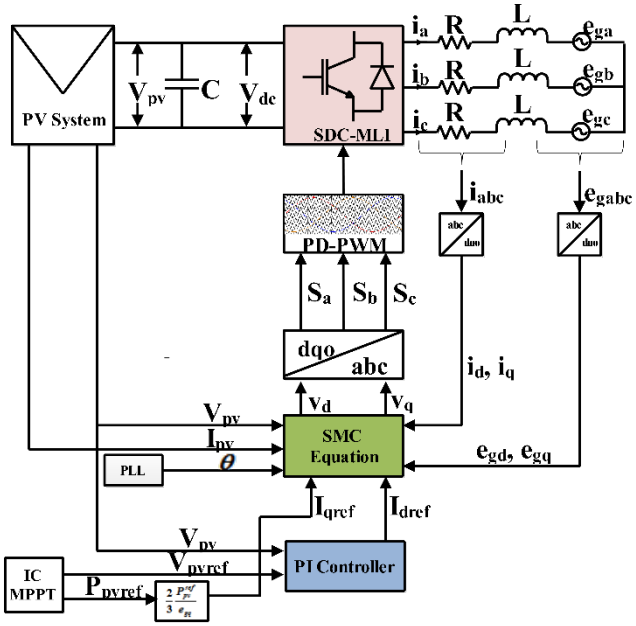

Fig. 2. Operational structure of the SSGCPV system

A PV system comprises 20 connected modules in series and 20 module in parallel each produces 38.05V, 5.15A rated voltage and current in a string. The dc link voltage of 761 V and current is 103A. Therefore PV system output power is ≈80 KW. The SDC-MLI circuit having 6 dc link capacitors each of 3300 µF, line resistance of 0.01 Ω and ac side inductance is

5 mH. The grid is operating at a potency of 660V at 50Hz frequency. The following PV panel specifications are considered, data from TN-72-5M195[33], the maximum panel output power is 195W, the voltage at maximum power 38.05V, current at maximum power 5.15 A, the open circuit (OC) voltage 43.5 V and short circuit current (SC) is 5.36 A.

The function of the PV system is monitored on the basis of the I-V and P-V characteristics, under different environmental conditions, like irradiation and temperature. The solar pinnacle radiation is 1000W / m^2, and the standard temperature test condition (STTC) is 25^0C. The I-V and P-V characteristics are displayed at different irradiations and temperatures as shown in Fig .3 and Fig .4.

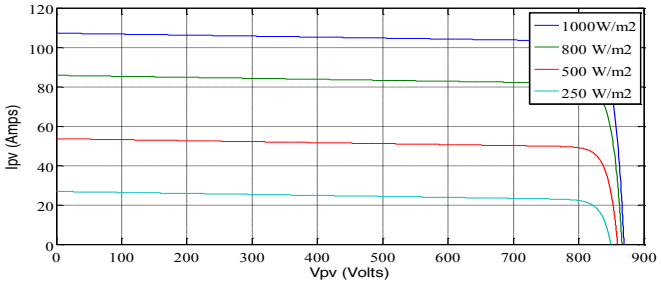

(a)

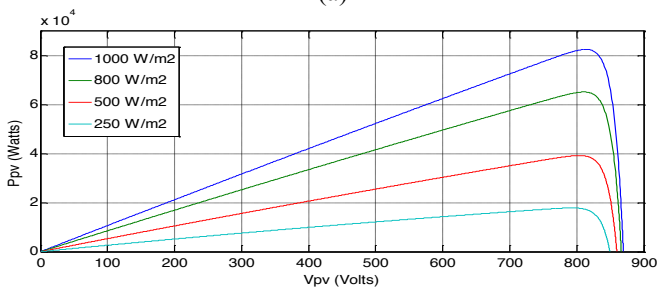

(b)

Fig. 3.(a). I-V and **(b)** P-V Characteristics of PV at distinct irradiations.

The observations made on the I-V and P-V characteristics at distinct operating conditions as changing irradiation and temperature on PV system. I-V and P-V characteristics at changing irradiation as shown in the Fig 3. To study the PV system working ability a distinct irradiations are applied. The standardized testing irradiation of PV system is 1000 W/m^2 , at which the obtained output current, voltage and power are the rated values. If any variation of irradiation such as 800 W/m^2 , 500 W/m^2 and 250 W/m^2 the output current , voltage and power are decreased.

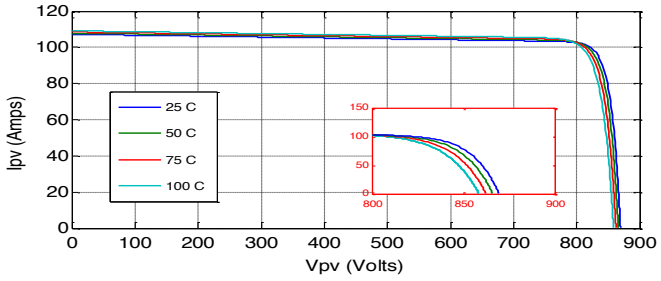

(a)

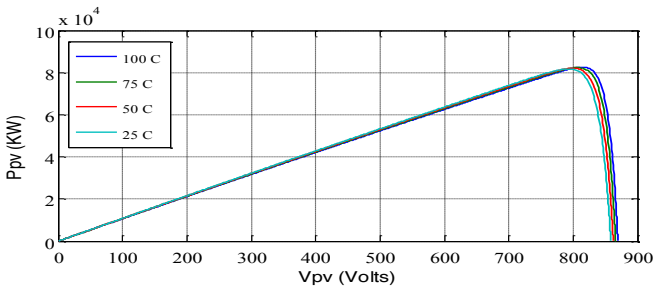

(b)

Fig. 4. (a). I-V and **(b)** P-V Characteristics of PV at distinct temperatures

The working ability of PV system at different temperatures as shown in the Fig.4. The standard working temperature of the PV system is 25^0C at which the obtained output current, voltage and power are rated values as shown in the I-V and P-V characteristics of Fig.4. If applied temperature is more than that of 25^0C the output current is increased, voltage is decreased and maximum power is not attained its rated value.

The PI-SMC controller's performance is analyzed and compared with the PI-PI, not shown, on Single-stage Grid connected Seven-level Diode clamped Photovoltaic (SGSDPV) system with the following cases:

4.1. Performance with standard atmospheric condition (SAC):

In SGSDPV system may not produce the required output voltage and current in open loop system and are also deviated from its nominal values even in closed loop system without using a controller because of external disturbances and nonlinearity of the system. The linear PI-PI controller may not give the desired expectations in operation due to the non-linear characteristics of the PV system. The SMC is a nonlinear controller and will provide effective outcome to reduce the uncertainties on the system, which will improve the system performance.The PI-SMC is designed and performed as a robustness to deliver the maximum power into the grid and dynamically responds from uncertainties and external disturbances. In this case, the system is simulated under SAC, the comparative observations for PI-PI and PI-SMC are presented in simulation results and numerical table as shown in Fig.5 and Table.2. The following observations are recorded under SAC as grid voltage and current, real power, reactive power, power factor and dc-link voltage settling time.

At SAC, the nominal values of solar radiation (1000 W/m^2) and temperature (25^0 C) are applied, as seen in Fig.5. In Fig.5 (a) shows the dc link voltage of 761 V obtained for both the cases but settling time is distinct to each other as shown in Table 2. Fig.5(b) & (c) displays grid voltage and current for PI-SMC and PI-PI, the grid current for PI-SMC is nearly in phase with voltage, but deviated in PI-PI. The power factor of PI-SMC and PI-PI based SGSDPV system is 0.9999 and 0.9854 as shown in Fig.5(f)., and also observe the real and reactive power variation of the system as shown in Fig.5(d) & (e).

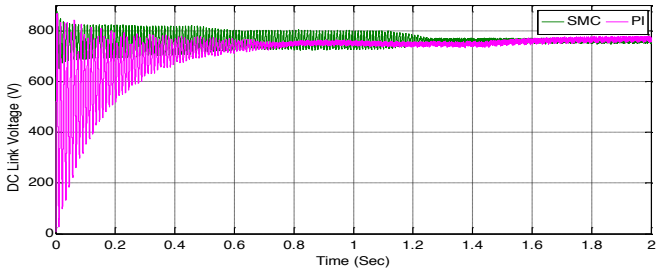

(a)

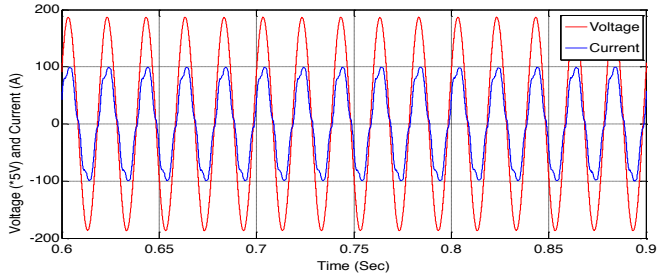

(b)

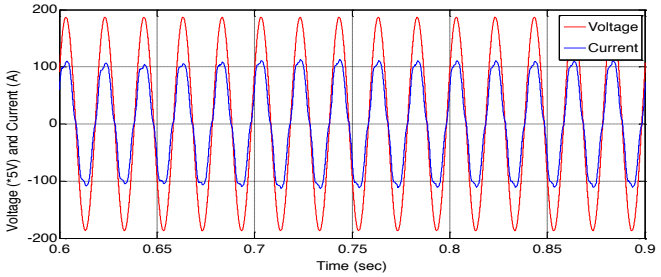

(c)

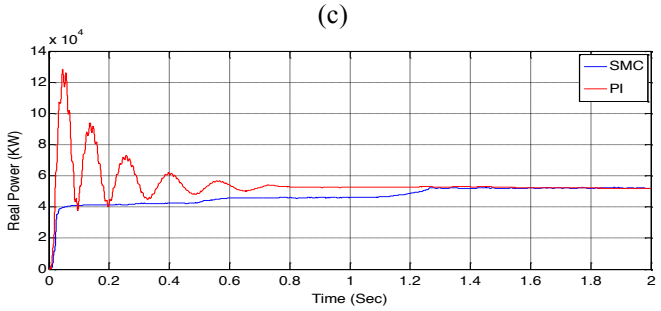

(d)

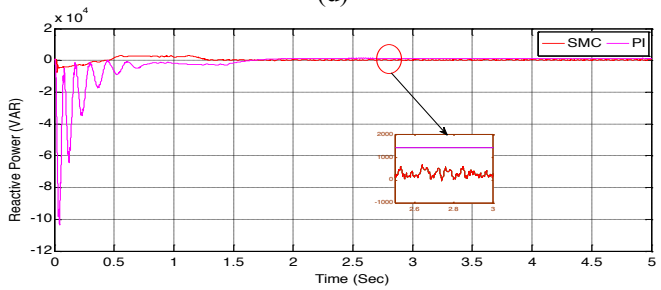

(e)

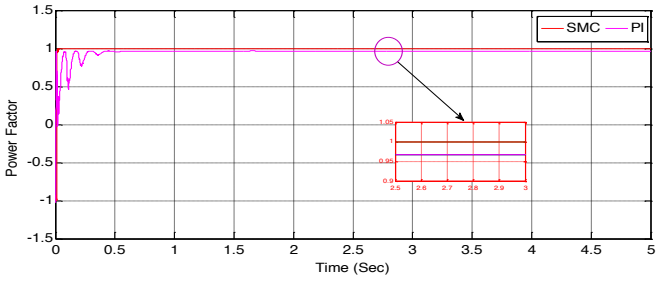

(f)

Fig. 5. Controllers comparision results under SAC (a) dc link voltage (b) grid voltage and current for PI-SMC (c) grid voltage and current for PI-PI (d) real power (e) reactive power (f) power factor

4.2. Performance with Changing Atmospheric Condition (CAC):

The irradiation and temperature at the input of the PV system are constant at SAC, but in practice, the input parameters of the PV system have been changed because of change in atmospheric condition. Equation (24) shows the control inputs of SMC is designed based on the external disturbances, uncertainties and nonlinearity of the system. It is necessary to transfer the maximum power into the grid-connected PV system and keep up the power factor near by the unity even in CAC. In CAC, the solar irradiation is changed from 100% to 70% at 0.5 sec to 0.85 sec and controller's comparison results are displayed on Fig.6.

In Fig. 6 (a) shows the dc-link voltage under the variation of irradiation from 0.5 sec to 0.85 sec, it is observed that the PI-SMC controller gave the best performance over the conventional PI-PI. The grid voltage and current waveforms for PI-SMC and PI-PI as shown in the Fig. 6(b) & (c), during the radiation change, the PI- SMC performs stable operation but the linear PI-PI makes the operation unstable.The designed controller maintains operation of the system as unity power factor as shown in Fig.6 (f) and real and reactive power s are stabilized after CAC as shown in Fig. (6) (d) & (e). The recorded observations of SAC and CAC as shown in Table 2.

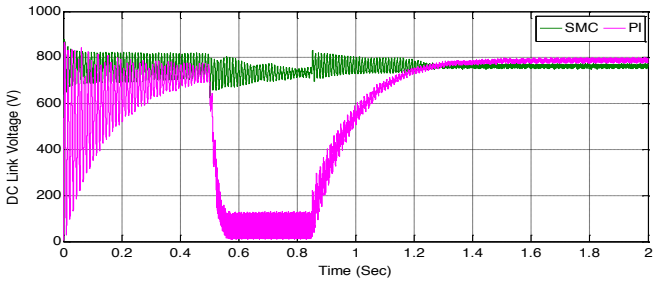

(a)

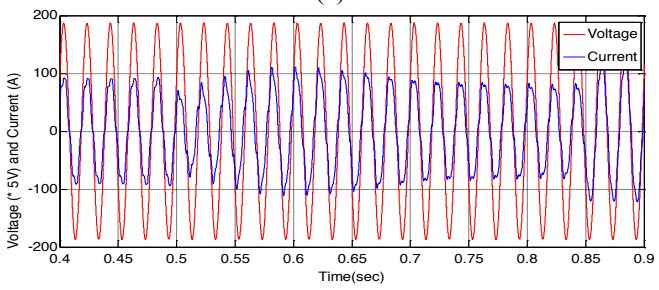

(b)

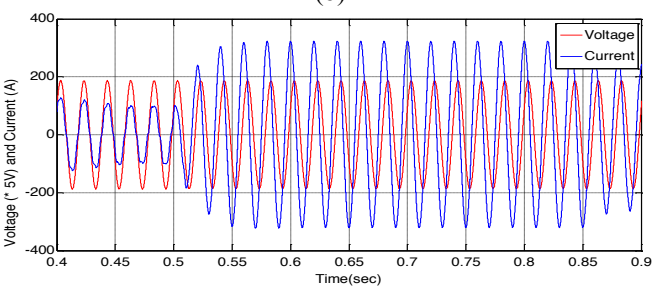

(c)

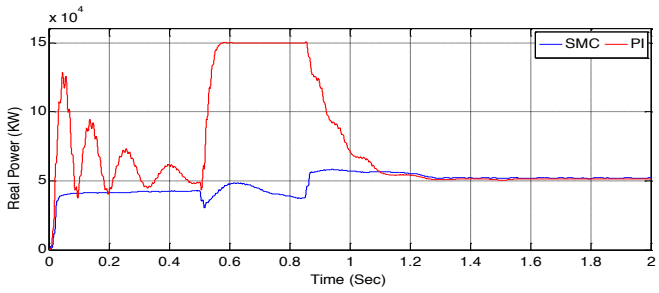

(d)

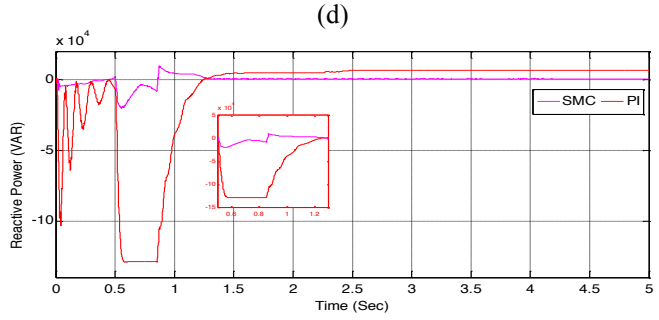

(e)

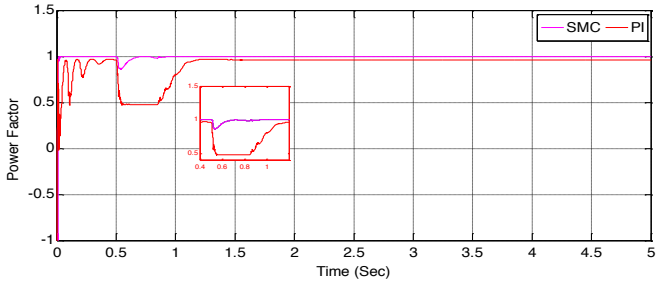

(f)

Fig. 6. Controllers comparision results under CAC (a) dc link voltage (b) grid voltage and current for PI-SMC (c) grid voltage and current for PI-PI (d) real power (e) reactive power (f) power factor.

From Table.2, it is noted that the PI-SMC gave the robust operation by comparing the PI-PI. In CAC, the variation of irradiation is applied from 0.5 seconds to 0.85 seconds in total running time. The dc link voltage settling time, in the above table, displayed after irradiation is recovered, i.e., at 0.85 sec. When radiation is recovered, the DC link voltage is stabilized within 0.4 second, it is why PI-SMC performs as a robust controller as compared with PI-PI.

In Fig.5 and Fig.6, the comparison analysis is done in the form of simulation and numerical in between PI-SMC and PI-PI. Results of PI-SMC shown better performance quantitatively in terms of

- Dc link voltage settling time is improved by 25% and 45% at SAC and CAC.
- Grid current is improved under CAC by 6.3%
- Reactive power is decreased up to 59.16%
- Power factor is improved by 1.63%

4.3. Performance with Three Phase Short Circuit Fault Analysis:

A three phase fault create the disruption in a power system. In this study, the performance of the controllers are estimated by applying a symmetrical fault at the grid side.

A fault is occured at 0.5 sec and cleared at 0.85 sec. The grid voltage during the fault is zero and under this fault current rises as shown in Fig.7 (b) and (c). After the fault clearance, the PI-SMC controller quickly reacts and current is settled at 0.85 sec, but in PI-PI controller will give unstable operation even after stipulated fault time and current is settled at 1.2 sec, as shown in Fig.7 (c). The real power is unstable during the fault because of three phase voltage is collapse and stabilized after fault clearence of 0.85 sec, as shown in Fig. 7(d). The PI-SMC maintain the power factor as near by unity before and after the fault as shown in Fig.7(f), but in PI-PI, there is a phase difference existing between them. The reactive power and dc link voltage variations, as shown in Fig.7. (a) & (e).

Table 2. Numerical observations of PI-PI and PI-SMC at SAC and CAC conditions

Operating Conditions	Grid Voltage (V) & Current (A) (RMS Values)		Real Power (W)		Reactive Power (VAR)		Apparent Power (VA)		Power Factor		DC link voltage settling time	
	PI-PI	PI-SMC	PI-PI	PI-SMC	PI-PI	PI-SMC	PI-PI	PI-SMC	PI-PI	PI-SMC	PI-PI	PI-SMC
SAC	660 & 79	660 & 79	51940	52070	1408	575	51960	52070	0.9854	0.9999	0.8sec	0.6sec
CAC	660 & 226*, 74**	660 & 56*, 79**	50410	52100	6543	434	50830	52100	0.9843	0.9999	0.55sec	0.4sec

* During the irradiation changing period i.e. 0.5 sec to 0.85 sec
** During the total running period

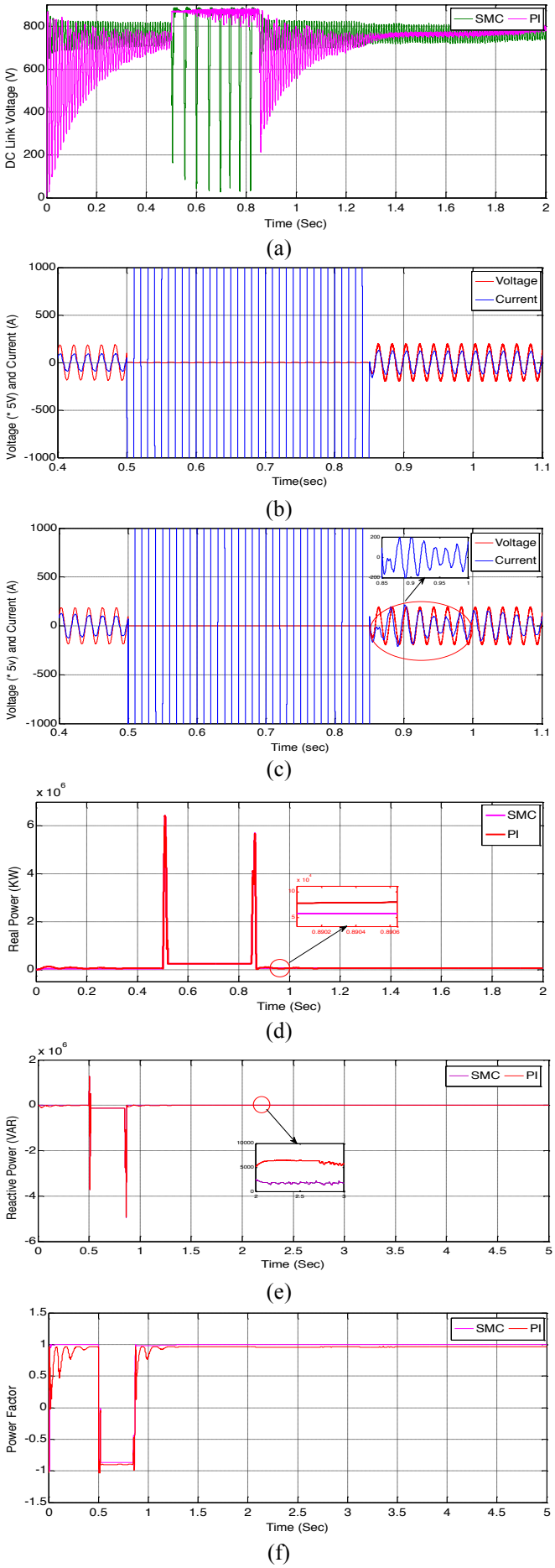

Fig. 7. Controllers comparision results under three phase short circuit fault (a) dc link voltage (b) grid voltage and current for SMC (c) grid voltage and current for PI (d) real power (e) reactive power (f) power factor

5. Conclusion:

The performance of single stage grid connected photovoltaic system with seven level diode clamped inverter is investigated through simulation with different combinations of controllers as proportional integral-proportional integral and proportional integral-sliding mode controller under the multiple scenarios's. The achievement of the proposed proportional integral-sliding mode controller effectively enhanced the dynamic stability of the system perfomance under the standard atmospheric condition, changing atmospheric condition and three phase fault occurrence. The simulation results shown the robustness of the proposed controller, reduces the settling time of the dc-link voltage which intern provides better power balance in between the photovoltaic system and grid. The results also shown the enhancement of the grid current, which is in phase with voltage to maintain nearer the unity power factor, it also reduces the reactive power. Furthermore, incremental conductance algorithm is added advantage for maximum power point tracking, because it provides a reference voltage to maintain power synchronization between the photovoltaic system and the grid.

References

[1] M. Shayestegan, "Overview of grid-connected two-stage transformer-less inverter design," *J. Mod. Power Syst. Clean Energy*, vol. 6, no. 4, pp. 642–655, 2018.

[2] D. G. Montoya, C. A. Ramos-Paja, and R. Giral, "Improved Design of Sliding-Mode Controllers Based on the Requirements of MPPT Techniques," *IEEE Trans. Power Electron.*, vol. 31, no. 1, pp. 235–247, 2016.

[3] Y. Yang and H. Wen, "Adaptive perturb and observe maximum power point tracking with current predictive and decoupled power control for grid-connected photovoltaic inverters," *J. Mod. Power Syst. Clean Energy*, vol. 7, no. 2, pp. 422–432, 2019.

[4] A. Merabet, L. Labib, A. M. Y. M. Ghias, A. Aldurra, and M. Debbouza, "Electrical Power and Energy Systems Dual-mode operation based second-order sliding mode control for grid- connected solar photovoltaic energy system," *Electr. Power Energy Syst.*, vol. 111, no. April, pp. 459–474, 2019.

[5] D. Menaga and V. Sankaranarayanan, "Performance comparison for grid connected photovoltaic system using sliding mode control," *J. King Saud Univ. - Eng. Sci.*, no. xxxx, pp. 0–7, 2020.

[6] W. Nsengiyumva, S. G. Chen, L. Hu, and X. Chen, "Recent advancements and challenges in Solar Tracking Systems (STS): A review," *Renew. Sustain. Energy Rev.*, vol. 81, no. June 2017, pp. 250–279, 2018.

[7] Menaga. D. and Sankaranarayanan. V., "A novel nonlinear sliding mode controller for a single stage grid-connected photovoltaic system," *ISA Trans.*, no. xxxx, 2020.

[8] B. Guo, M. Su, Y. Sun, H. Wang, B. Liu, X. Zhang, J.

Pou, Y. Yang, and P.Davari, "Optimization Design and Control of Single-Stage Single-Phase PV Inverters for MPPT Improvement," *IEEE Trans. Power Electron.*, vol. 35, no. 12, pp. 13000–13016, 2020.

[9] Y. Chaibi, A. Allouhi, M. Salhi, and A. El-jouni, "Annual performance analysis of different maximum power point tracking techniques used in photovoltaic systems," *Prot. Control Mod. Power Syst.*, vol. 4, no. 1, pp. 1–10, 2019.

[10] A. Ahmad, N. Ullah, N. Ahmed, A. Ibeas, G. Mehdi, J. Herrera, and A. Ali, "Robust Control of Grid-tied Parallel Inverters using Nonlinear Backstepping Approach," *IEEE Access*, vol. 7, pp. 111982–111992, 2018.

[11] M. Aourir, A. Abouloifa, I. Lachkar, C. Aouadi, and F. Giri, "Nonlinear control and stability analysis of single stage grid-connected photovoltaic systems," *Electr. Power Energy Syst.*, vol. 115, no. June 2019, p. 1-15, 2020.

[12] A. Alhejji, "Capability enhancement of DC-link voltage in a single-stage grid-connected photovoltaic power system," *Int. J. Renew. Energy Res.*, vol. 10, no. 1, pp. 474–485, 2020.

[13] A. Ismail, M. Ali, M. A. Sayed, and T. Takeshita, "Isolated single-phase single-stage DC-AC cascaded transformer-based multilevel inverter for stand-alone and grid-tied applications," *Int. J. Electr. Power Energy Syst.*, vol. 125, April 2020, pp. 1-15, 2021.

[14] P. K. Sahu and M. D. Manjrekar, "Controller design and implementation of solar panel companion inverters," *IEEE Trans. Ind. Appl.*, vol. 56, no. 2, pp. 2001–2011, 2020.

[15] E. Kabalcı, "Review on novel single-phase grid-connected solar inverters: Circuits and control methods," *Sol. Energy*, vol. 198, pp. 247–274, 2020.

[16] A. Jendoubi, F. Tlili, and F. Bacha, "Sliding mode control for a grid connected PV-system using interpolation polynomial MPPT approach," *Math. Comput. Simul.*, vol. 167, no. xxxx, pp. 202–218, 2020.

[17] F. F. Ahmad, C. Ghenai, A. K. Hamid, and M. Bettayeb, "Application of sliding mode control for maximum power point tracking of solar photovoltaic systems: A comprehensive review," *Annu. Rev. Control*, no. xxxx, 2020.

[18] C. Dang, X. Tong, and W. Song, "Sliding-Mode Control in dq-Frame for a Three-Phase Grid-Connected Inverter with LCL-Filter," *J. Franklin Inst.*, 2020.

[19] J. A. Cortajarena, O. Barambones, P. Alkorta, and J. De Marcos, "Sliding mode control of grid-tied single-phase inverter in a photovoltaic MPPT application," *Sol. Energy*, vol. 155, pp. 793–804, 2017.

[20] H. Myneni and S. K. Ganjikunta, "Energy Management and Control of Single-Stage Grid-Connected Solar PV and BES System," *IEEE Trans. Sustain. Energy*, vol. 11, no. 3, pp. 1739–1749, 2020.

[21] B. Li, Y. Liang, G. Wang, H. Li, and J. Ding, "A control strategy for soft open points based on adaptive voltage droop outer-loop control and sliding mode inner-loop control with feedback linearization," *Int. J. Electr. Power Energy Syst.*, vol. 122, no. January, p. 106205, 2020.

[22] Y. Chaibi, M. Salhi, and A. El-Jouni, "Sliding mode controllers for standalone PV systems: Modeling and approach of control," *Int. J. Photoenergy*, vol. 2019, no. Ic, 2019.

[23] A. Kihal, F. Krim, A. Laib, B. Talbi, and H. Afghoul, "An improved MPPT scheme employing adaptive integral derivative sliding mode control for photovoltaic systems under fast irradiation changes," *ISA Trans.*, vol. 87, pp. 297–306, 2019.

[24] M. A. Mahmud, M. J. Hossain, S. Member, H. R. Pota, and N. K. Roy, "Robust Nonlinear Controller Design for Three-Phase Grid-Connected Photovoltaic Systems Under Structured Uncertainties," *IEEE Trans. Power Delivery* ,vol. 29, no. 3, pp. 1221–1230, 2014.

[25] M. A. Mahmud, H. R. Pota, M. J. Hossain, S. Member, and N. K. Roy, "Robust Partial Feedback Linearizing Stabilization Scheme for Three-Phase Grid-Connected Photovoltaic Systems," *IEEE J. Phot.* vol. 4, no. 1, pp. 423–431, 2014.

[26] K. R. Reddy, V. N. Reddy, and M. V. Kumar, "Control of Single Stage Grid Tied Photovoltaic Inverter Using Incremental Conductance Method," *International Journal of Power Electronics and Drive Systems,* vol. 9, no. 4, pp. 1702–1708, 2018.

[27] K. R. Reddy, V. N. Reddy, and M. V Kumar, "Improved Robust Controller Design for Stabilization of Grid-Tied Photovoltaic System," *Journal of Sci. and Industrial Res.,* vol. 78, no. July, pp. 431–436, 2019.

[28] A. Mehta and B. Naik, "Sliding Mode Controllers for Power Electronic Converters," *Springer Nature*, vol. 534. 2019.

[29] P. R. Bana, K. P. Panda, S. Padmanaban, L. Mihet-Popa, G. Panda, and J. Wu, "Closed-Loop Control and Performance Evaluation of Reduced Part Count Multilevel Inverter Interfacing Grid-Connected PV System," *IEEE Access*, vol. 8, pp. 75691–75701, 2020.

[30] K. R. Reddy, V. N. Reddy, M. V. Kumar, and S. K. Tummala, "Configurations and Control Strategy of a Single Stage Grid Connected PV System," *E3S Web Conf.*, vol. 184, p. 01074, 2020.

[31] P. K. Sahu and M. D. Manjrekar, "Controller design and implementation of solar panel companion inverters," *IEEE Trans. Ind. Appl.*, vol. 56, no. 2, pp. 2001–2011, 2020.

[32] M. Spieler, O. Vanegas, and G. Marek, "Performance analysis of decoupling DC-link capacitors for a SiC-MOSFET-inverter module," *8th Int. Conf. Renew. Energy Res. Appl. ICRERA 2019*, pp. 200–205, 2019.

[33] M. Oumaima, T. Mouhavdine, F. M. Janeiro, H. Abdeloawahed, and K. Khalid, "Estimation of photovoltaic panel parameters by a numerical heuristic searching algorithm," *8th Int. Conf. Renew. Energy Res. Appl. ICRERA 2019*, pp. 401–406, 2019.

[34] Abdelhakim Belkaid, Ilhami Colak, Korhan Kayisli, and Ramazan Bayindir, "Design and Implementation of a Cuk Converter Controlled by a Direct Duty Cycle INC-MPPT in PV Battery System," *Int. J. Smart Grid*, vol. 3, no. 1, pp. 19–25, 2019.

[35] A. Belkaid, I. Colak, K. Kayisli, and R. Bayindir, "Indirect Sliding Mode Voltage Control of Buck Converter," *8th Int. Conf. on Smart Grid.* icsmartgrid *2020,* no. 2, pp. 90–95, 2020.

[36] K. E. Okedu, A. Al Senaidi, I. Al Hajri, I. Al Rashdi, and W. Al Salmani, "Real Time Dynamic Analysis of Solar

PV Integration for Energy Optimization," *Int. J. Smart Grid,* vol. 4, no. 2, pp. 68–79, 2020.

[37] T. T. Guingane, D. Bonkoungou, E. Korsaga, E. Simonguy, Z. Koalaga, and F. Zougmore, "Modeling and Simulation of a Photovoltaic System Connected to The Electricity Grid with MALTAB/Simulink/Simpower Software," *8th Int. Conf. on Smart Grid.* icsmartgrid *2020,* pp. 163–168, 2020.